

Branching Subset Simulation

Hugh J. Kinnear^a, F.A. DiazDelaO^a

^a*Clinical Operational Research Unit, Department of Mathematics, UCL, London, WC1H 0BT, United Kingdom*

Abstract

Subset Simulation is a Markov chain Monte Carlo method, initially conceived to compute small failure probabilities in structural reliability problems. This is done by iteratively sampling from nested subsets in the input space of a performance function. Subset Simulation has since been adapted as a sampler in other realms such as optimisation, Bayesian updating and history matching. In all of these contexts, it is not uncommon that either the geometry of the input domain or the nature of the corresponding performance function cause Subset Simulation to suffer from ergodicity problems. To address these problems, this paper proposes Branching Subset Simulation. The proposed framework dynamically partitions the input space, and recursively begins Branching Subset Simulation anew in each partition. It is shown that Branching Subset Simulation is less likely than Subset Simulation to suffer from ergodicity problems and has improved sampling efficiency in the presence of multi-modality.

Keywords: Subset simulation, Markov chain Monte Carlo, Community detection, Reliability analysis, Support vector machine classification, Unconstrained global optimization

1. Introduction

A wide range of important problems in applied and computational mathematics can be solved using algorithms that sample from a *set of interest*. Some notable examples include the following problems: (i) estimating the probability of failure of an engineering system. Structural reliability analysis solves this by sampling from the failure set, i.e. the set of input combinations for which the output of a model of the system exceeds a critical threshold; (ii) determining how a statistical hypothesis is updated by observing data. Bayesian inference solves this by sampling from the support of a posterior probability density function; (iii) finding the local/global optima of a function. Numerical optimisation solves this by sampling from the neighbourhood of local and global optimisers; (iv) matching computer model output to experimental data. Some calibration strategies solve this by sampling from a set of input values for which the model output is close to a target level, measured with a suitable metric.

Even if the seemingly disparate problems (i)-(iv) belong to different disciplines, it is possible to describe them under one formal framework. Let $g: \mathbb{R}^d \rightarrow \mathbb{R}$ be a *performance function* that assigns a scalar to each point in the *input space* \mathbb{R}^d . Let $f(\cdot)$ be a probability density function defined on the input space, called the *input distribution*. An *exceedance region* F is defined by a threshold $b \in \mathbb{R}$, such that $F = \{\mathbf{x} \in \mathbb{R}^d : g(\mathbf{x}) \geq b\}$. By selecting the appropriate performance function and threshold, the set of interest of reliability analysis [1], Bayesian inference [2–5], optimisation [6], and calibration through history matching [7] can be modeled as an exceedance region. With these definitions, several types of analyses can be thought of as estimating the statistical properties of their corresponding exceedance region. For instance, estimating the relative size of F with respect to the input space \mathbb{R}^d by producing samples from $f(\cdot)$ provides an estimate of the *exceedance probability*,

$$P_F = \int_{\mathbb{R}^d} \mathbb{1}_F(\mathbf{x}) f(\mathbf{x}) d\mathbf{x}. \quad (1)$$

Estimating P_F can be extremely challenging, since high dimensionality of the input space and small exceedance probabilities are not uncommon in applications. This can severely hinder the sampling from F . In

order to cope with these difficulties, Subset Simulation (SuS) was originally designed for estimating probabilities of failure in reliability analysis [1]. In this context, the performance function $g(\cdot)$ describes the response of a physical system to inputs such as geometry, material properties and loadings, to name a few.

SuS is a variance reduction technique that explores the input space using Markov chain Monte Carlo (MCMC). It can be seen as a greedy algorithm, since it always exploits the current highest performing regions of the input space, as measured by the performance function $g(\cdot)$. Due to this, it has been shown [8] that SuS can suffer from ergodicity problems causing the estimator for exceedance probabilities to return inaccurate results. The counterexamples presented in [8] have motivated the creation of new algorithms that address the problem by exploring the input space more effectively. For instance, fitness-based seed selection [9] promotes exploration of lower performing regions by re-weighting the starting seeds of the Markov chains. Sequential space conversion [10] constructs control variates which can provide global information about the performance function. Spectral embedding-based reliability methods [11] build a surrogate performance function and partition of the parameter space which highlight important regions.

Given the number of contexts in which SuS can be applied, such as the ones described by problems (i)-(iv), and to contribute to the search of efficient samplers, this paper proposes a general framework based on SuS called Branching Subset Simulation (BSuS). The main idea is to dynamically partition the input space and then restart the algorithm recursively in each set of the partition. Promising regions of the input space that SuS would otherwise ignore have a greater chance of being explored because of this partitioning strategy. This idea can be implemented without relying on a specific surrogate model, or at the cost of losing the important statistical properties guaranteed by SuS. Additionally, BSuS is naturally parallelisable, and the parameters of each parallel run can be adjusted independently, resulting in greater sampling efficiency. BSuS does require additional user specified parameters, but it is shown with numerical examples that it outperforms SuS for a wide range of parameter values.

The paper is organised as follows. Section 2 gives an overview of the original SuS algorithm. BSuS and the BSuS estimator are introduced in Section 3. The strategy for partitioning the input space is discussed in Section 4. In Section 5, numerical examples tackling ergodicity and multi-modality are presented. The paper is concluded in Section 6.

2. Subset Simulation

2.1. The Original Algorithm

To estimate exceedance probabilities, the original SuS algorithm models exceedance regions using a nested sequence of *intermediate exceedance regions*, called *intermediate failure sets* in the structural reliability context, $F_m \subseteq F_{m-1} \subseteq \dots \subseteq F_1 \subseteq F_0 = \mathbb{R}^d$. The idea is to sequentially approximate a rare event using relatively frequent events which are easier to sample from. Each intermediate exceedance region has an associated *level* contained within it, where a level is a member of the set $\mathcal{L} = \{\mathbf{X} \subset \mathbb{R}^d : |\mathbf{X}| = n\}$ and $n \in \mathbb{N}$ is the *level size*.

The *initial level*, \mathbf{X}^0 , is created by sampling n times from the input distribution. The performance function $g(\cdot)$ is then evaluated at each sample in the the initial level. The top $n_c = np$ performing samples are chosen as *seeds* for the next level, where the *level probability* $p \in (0, 1]$ is a parameter chosen by the modeller. Note that this requires n and p to be chosen such that n_c is an integer. The performance of the lowest performing seed becomes the first *intermediate threshold* b_1 , which defines the first intermediate exceedance region $F_1 = \{\mathbf{x} \in \mathbb{R}^d : g(\mathbf{x}) \geq b_1\}$. A Markov chain of length $n_s = p^{-1}$, with stationary distribution $f(\mathbf{x})\mathbb{1}_{F_1}(\mathbf{x})$, is then created from each of the seeds. Again, note that p must be chosen so that n_s is an integer. The Markov chains taken together comprise the next level, \mathbf{X}^1 . The process is repeated to create all subsequent levels. Namely, to create \mathbf{X}^k , seeds are chosen from \mathbf{X}^{k-1} . The seeds define an intermediate threshold b_k and an intermediate exceedance region F_k . The level is then created from the seeds using Markov chains with a stationary distribution of $f(\mathbf{x})\mathbb{1}_{F_k}(\mathbf{x})$. This process continues until a stopping condition is met. The output of the algorithm is the sequence of levels it creates, $(\mathbf{X}^k)_{k=0}^m$.

Many different Markov chain strategies have been proposed for SuS [12, 13]. The standard Metropolis algorithm struggles in high dimensions [14] and so the examples in this paper use the Modified Metropolis

algorithm [1] which is summarised in Algorithm 1. The examples in this paper use a standard normal distribution as the proposal distribution. This algorithm takes advantage of the special structure of the probability density functions which SuS targets, and so it is able to have good sampling efficiency in high dimensions. To reflect the different possible choices for a Markov chain algorithm, a generic notation for the step function will be used: $\text{STEP}_f : \mathbb{R}^d \rightarrow \mathbb{R}^d$, where f is the stationary distribution of the Markov chain. Given a starting sample $\mathbf{x} \in \mathbb{R}^d$, the next member of the chain will be denoted as $\text{STEP}_f(\mathbf{x})$. The structure of the stationary distribution in Algorithm 1 assumes independence between the inputs. This is due to the convention of assuming the input distribution is a standard multivariate normal, which is justified by altering the performance function appropriately depending on the available description of the input distribution. For instance, if the input distribution is explicitly known, then the Rosenblatt transformation [15] can be applied. Alternatively, if only the marginal distributions and correlations are given the joint probability distribution can be approximated by a Nataf distribution [16].

Algorithm 1 Modified Metropolis

Input

Candidate: $\mathbf{x} \in \mathbb{R}^d$

Target distribution: $f(\mathbf{x}) = \mathbb{1}_F(\mathbf{x}) \prod f_i(x_i)$

Proposal distribution: $q(\cdot|\mathbf{x})$

```

1: procedure MODIFIEDMETROPOLIS( $\mathbf{x}$ )
2:   for  $1 \leq i \leq d$  do
3:     Sample  $x'_i \sim q(\cdot|x_i)$ 
4:      $\theta \leftarrow \min(1, f(x'_i)/f(x_i))$ 
5:      $\alpha \leftarrow \text{BERNOULLI}(\theta)$ 
6:     if  $\alpha = 0$  then
7:        $x'_i \leftarrow x_i$ 
8:    $\mathbf{x}' \leftarrow (x'_1, \dots, x'_d)$ 
9:   if  $\mathbb{1}_F(\mathbf{x}) = 0$  then
10:     $\mathbf{x}' \leftarrow \mathbf{x}$ 
11:  return  $\mathbf{x}'$ 

```

The choice of stopping condition is context dependent. In reliability analysis (the original application of SuS) there is a specified performance threshold b_* which defines an exceedance region F_* called the *failure region*. In this context, the goal is to estimate the *probability of failure*, which is the exceedance probability of the failure region, and so the algorithm should only be stopped once enough samples have been produced in the failure region. Explicitly, the algorithm stops on level m if

$$\sum_{\mathbf{x} \in \mathbf{X}^m} \mathbb{1}_{F_*}(\mathbf{x}) \geq n_c. \quad (2)$$

In other contexts where SuS is used, such as Bayesian updating [3], a predefined threshold might not exist. In those cases, some type of convergence criteria is used instead. For instance, the algorithm could stop if the performance of all samples in a level is constant. Again, to reflect the potential for different possible stopping conditions, a generic notation will be used: $\text{STOP} : \mathcal{L} \rightarrow \{\mathbf{True}, \mathbf{False}\}$. The complete SuS procedure is summarised in Algorithm 2.

2.2. Estimating Exceedance Probabilities

The output levels of SuS can be used to estimate any exceedance probability P_F defined by a threshold b and exceedance region F . Let $b_0 = -\infty$ and $m' = \max(\{k : b_k < b\})$. Since $F \subseteq F_{m'} \subseteq \dots \subseteq F_1 \subseteq F_0$, the product rule can be used to obtain an expression for the exceedance probability:

$$P_F = \mathbb{P}(F_1|F_0)\mathbb{P}(F_2|F_1) \dots \mathbb{P}(F_{m'}|F_{m'-1})\mathbb{P}(F|F_{m'}). \quad (3)$$

Algorithm 2 Subset Simulation

InputLevel size: $n \in \mathbb{N}$ Level probability: $p \in (0, 1]$ Input distribution: $f: \mathbb{R}^d \rightarrow \mathbb{R}$ Performance function: $g: \mathbb{R}^d \rightarrow \mathbb{R}$ **Definitions** $n_c \leftarrow np$ $n_s \leftarrow p^{-1}$ **Subroutines**STOP: $\mathcal{L} \rightarrow \{\mathbf{True}, \mathbf{False}\}$ STEP: $\mathbb{R}^d \rightarrow \mathbb{R}^d$

```
1: procedure SUBSETSIMULATION
2:   Sample  $\mathbf{x}_1^0, \dots, \mathbf{x}_n^0 \sim f$ 
3:    $\mathbf{X}^0 \leftarrow (\mathbf{x}_i^0)_{i=1}^n$ 
4:    $m \leftarrow 0$ 
5:   while STOP( $\mathbf{X}^m$ ) is False do
6:     let  $\mathbf{x}'_1, \dots, \mathbf{x}'_n$  be a relabelling of  $\mathbf{X}^m$  such that  $g(\mathbf{x}'_1) \geq \dots \geq g(\mathbf{x}'_n)$ 
7:      $m \leftarrow m + 1$ 
8:      $b_m \leftarrow g(\mathbf{x}'_{n_c})$ 
9:      $F_m \leftarrow \{\mathbf{x} \in \mathbb{R}^d : g(\mathbf{x}) \geq b_m\}$ 
10:     $f_m(\mathbf{x}) \leftarrow f(\mathbf{x}) \mathbb{1}_{F_m}(\mathbf{x})$ 
11:    for  $1 \leq i \leq n_c$  do
12:       $\mathbf{x}_{i,1}^m \leftarrow \mathbf{x}'_i$ 
13:      for  $2 \leq j \leq n_s$  do
14:         $\mathbf{x}_{i,j}^m \leftarrow \text{STEP}_{f_m}(\mathbf{x}_{i,j-1}^m)$ 
15:       $\mathbf{X}^m \leftarrow ((\mathbf{x}_{i,j}^m)_{i=1}^{n_c})_{j=1}^{n_s}$ 
16:  return  $(\mathbf{X}^k)_{k=0}^m$ 
```

It is therefore natural to estimate P_F as the product of estimators of each term in Equation 3. These estimators are denoted here as $\hat{P}_1, \hat{P}_2, \dots, \hat{P}_{m'+1}$. The following definition is kept general for convenience, but the case described above can be recovered by letting $m = m'$ and $F_{m+1} = F$.

Definition 1 (SuS Estimator). Given a nested sequence of sets $F_0, F_1, \dots, F_m, F_{m+1}$ and a sequence of levels $\mathbf{X}^0, \dots, \mathbf{X}^m$ each of size n , an estimator \hat{P} is a SuS estimator for $\mathbb{P}(F_{m+1}|F_0)$ with respect to the density function f if it has the following product form:

$$\hat{P} = \prod_{i=1}^{m+1} \hat{P}_i, \quad (4)$$

where $\hat{P}_i = \frac{1}{n} \sum_{\mathbf{x} \in \mathbf{X}^{i-1}} \mathbb{1}_{F_i}(\mathbf{x})$ and $\mathbf{x} \sim f|F_i$ for all \mathbf{X}^i .

For the rest of this section, the analysis is simplified by assuming that the intermediate thresholds are chosen a priori rather than dynamically, and that the samples generated by different chains are uncorrelated through the indicator functions. With these assumptions, it can be shown that SuS estimators are consistent and asymptotically unbiased [1]. Based on the sequence of levels $\mathbf{X}^0, \dots, \mathbf{X}^{m'}$ a SuS estimator can be used to estimate the required exceedance probability:

$$P_F = \mathbb{P}(F) = \mathbb{P}(F|F_0) \approx \hat{P}_F = \prod_{i=1}^{m'+1} \hat{P}_i = p^{m'} \hat{P}_{m'+1}, \quad (5)$$

where the last equality holds since $\hat{P}_k = p$ for $1 \leq k \leq m'$ due to the adaptive choice of intermediate thresholds.

It is straightforward to see that the first estimator in the product, \hat{P}_1 , is a direct Monte Carlo (DMC) estimator. The corresponding coefficient of variation (c.o.v) is given by:

$$\delta_1 = \sqrt{\frac{1 - P_1}{n P_1}}. \quad (6)$$

An estimation of the c.o.v, $\hat{\delta}_1$, can be made by substituting \hat{P}_1 for P_1 in Equation 6.

The rest of the estimators in the product in Equation 5 are MCMC estimators. Normally, Markov Chain methods require a burn-in period before the samples have the target distribution. SuS however has a property known as perfect sampling, where the seeds of the chains will always have been sampled according to the target distribution. This means that there is no burn-in period and all the samples can be used in the calculation. The c.o.v of the MCMC estimators is given by

$$\delta_k = \sqrt{\frac{1 - P_k}{n P_k} (1 + \gamma_k)}, \quad (7)$$

where γ_k is a factor accounting for the correlation between samples in the same chain. An estimator for the c.o.v., $\hat{\delta}_k$ for $2 \leq k \leq m' + 1$, can be obtained by substituting γ_k for an estimation $\hat{\gamma}_k$ and P_k for \hat{P}_k in Equation 7 [1].

Since the samples generated by Markov chains are correlated, MCMC estimators will have a higher c.o.v. than DMC estimators given the same number of samples. The *effective sample size* of an MCMC estimator is $n/(1 + \gamma_k)$. The higher the correlation of the chains, the lower the effective number of samples. A common estimator used for the c.o.v. of the SuS estimator δ is

$$\hat{\delta} = \sqrt{\sum_{k=1}^{m+1} \hat{\delta}_k^2}. \quad (8)$$

3. Branching Subset Simulation

3.1. Motivation

Regardless of the context in which SuS is applied, whether that is reliability analysis, Bayesian inference or optimisation, its effectiveness can be characterised as its ability to consistently sample from the important regions of the input space. Consider the neighbourhood of the *design point*, that is, the point in an exceedance region with the highest probability density. Any time SuS fails to populate this region, the resulting estimator will tend to underestimate the true exceedance probability since it contributes the most to the integral in Equation 1.

As discussed in the previous section, at any given level of a SuS run, the highest performing samples are chosen as seeds. SuS then defines the next level by exploring the input space in the neighbourhood of those seeds. This greedy approach is often a sensible course of action. However, there are cases where unimportant sets in lower exceedance regions become important in higher exceedance regions. Under these circumstances it is possible that SuS produces no seeds in the now important set.

The two-dimensional *piecewise linear function* described in [8] was constructed to highlight exactly this type of deficiency of the SuS algorithm. This performance function is given by

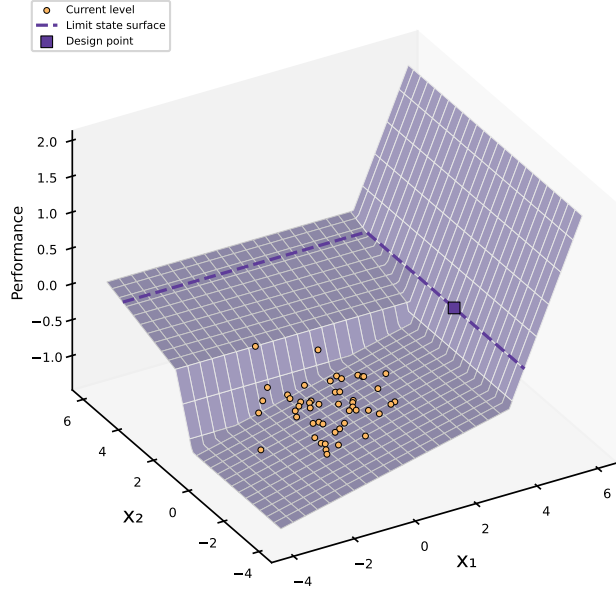
$$\begin{aligned} g(x) &= -\min(g_1(x), g_2(x)), \text{ where} \\ g_1(x) &= \begin{cases} 4 - x_1 & x_1 > 3.5, \\ 0.85 - 0.1x_1 & x_1 \leq 3.5, \end{cases} \\ g_2(x) &= \begin{cases} 0.5 - 0.1x_2 & x_2 > 2, \\ 2.3 - x_2 & x_2 \leq 2. \end{cases} \end{aligned} \quad (9)$$

For consistency, note that Equation 9 has been multiplied by -1 , since this paper uses the convention that SuS attains progressively higher intermediate thresholds. The goal in this context is to estimate the probability of failure where the failure region is defined by the threshold $b = 0$.

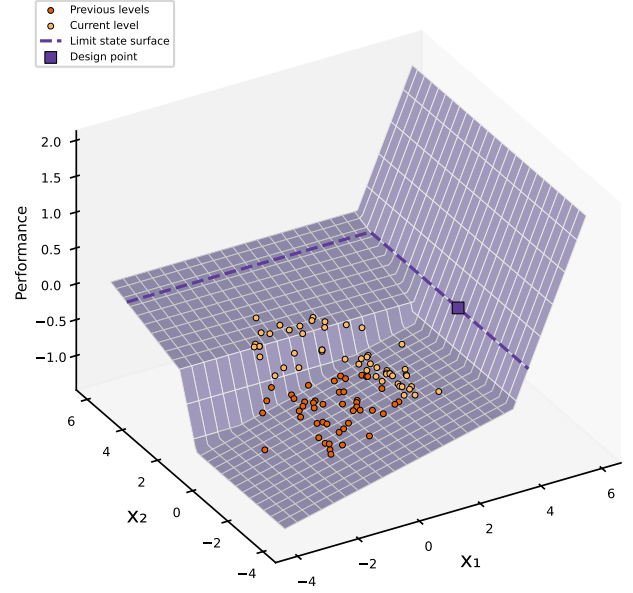
A single run of SuS using level size of $n = 500$, level probability of $p = 0.1$, and the stopping condition in Equation 2 is shown in Figure 1. Note that the *limit state surface* of a failure region is the set of points in the input space with performance equal to defining threshold of that failure region. In the region populated by the initial level, the highest performing samples are in the direction of positive x_2 , since it has steepest gradient, and so this is the direction in which SuS travels. However, further from the mean of the input distribution, the performance function begins to increase more rapidly in the direction of positive x_1 , meaning that ultimately this is where the design point is located. Eventually, SuS manages to produce some samples in the failure region and the stopping condition is satisfied. Despite this, the highest density area of the failure region has not been explored, and the probability of failure is severely underestimated. Since SuS is a stochastic algorithm, there will be runs where the neighbourhood of the design point will be sampled from. In those cases, however, the SuS estimator will tend to over estimate the probability of failure.

This behaviour leads to an undesirable statistical estimator. Figure 2 shows a kernel density estimate of the SuS estimator for the piecewise linear function built from 100 SuS runs. A reference probability of 3.2×10^{-5} was calculated using DMC with 10^8 samples. The figure shows a bimodal probability density function. This is unsurprising: the left mode corresponds to the 77 runs that do not populate the neighbourhood of the design point, whereas the right mode is the result of 23 runs that do. The empirical mean of all the estimators is 2.4×10^{-5} . Whilst this is a decent estimate of the reference probability, the variance of the SuS estimator is prohibitively large for practical purposes. Additionally, there is very little density in the neighbourhood of the reference probability itself, and so it is very unlikely that any individual SuS run will serve as a useful estimate for the exceedance probability.

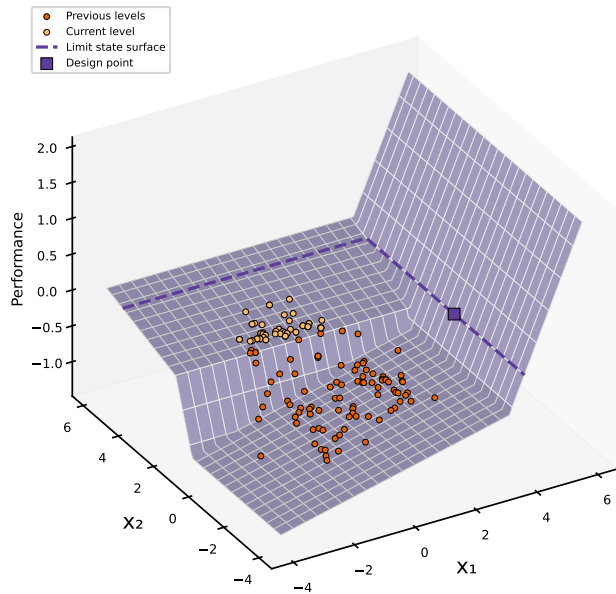
The simplest approach to overcoming these issues is to adjust the parameters of SuS. The number of seeds can be increased by either increasing the level size or the level probability. This will help since more seeds means more of the input space will be explored. Increasing the spread of the proposal distribution allows the chains to move between disparate regions of the input space more freely. Both of these approaches



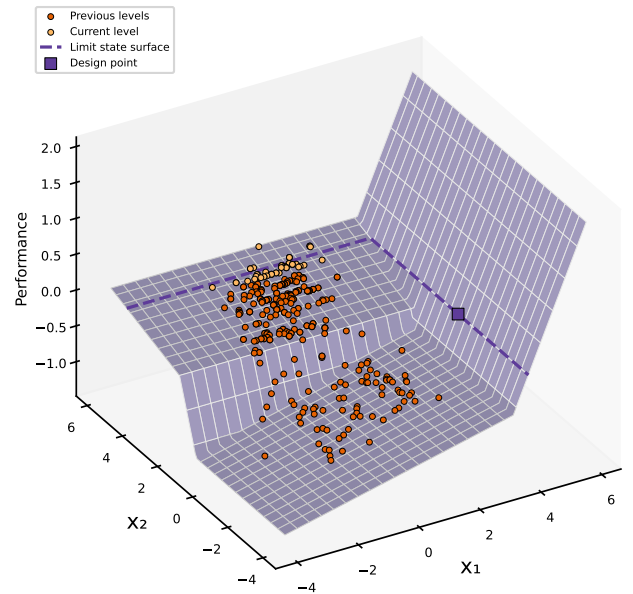
(a) Initial level



(b) Level 1



(c) Level 2



(d) Level 6

Figure 1: SuS running on the piecewise linear function. For clarity, only every 10^{th} sample has been plotted. SuS is lead away from the design point resulting in a poor estimate for the failure probability.

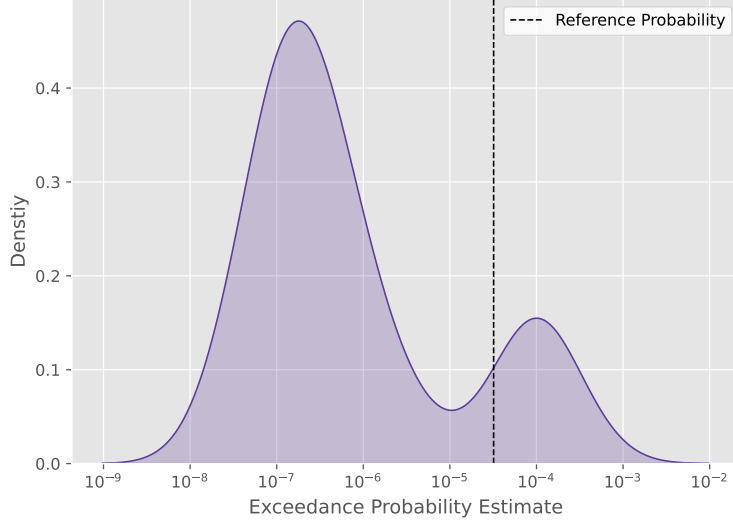


Figure 2: Kernel density estimate for 100 SuS exceedance probability estimators on the piecewise linear function, compared to a reference probability. The exceedance probability estimates are on a log scale.

share a fundamental flaw. In the case where the performance function is a black box, it is impossible to know a priori how these parameters should be adjusted. If the level size or level probability is too large, needless computational cost will be incurred. If the spread of the proposal distribution is too large, the correlation of the chains may increase which in turn causes the c.o.v. of the exceedance probability estimate to increase. To address all of these difficulties, this paper proposes BSuS.

3.2. Proposed Algorithm

BSuS is a general framework based on the original SuS algorithm that aims at improving the exploration of the input space. The idea is to create a partition of the input space at each level. Then, in each set of the partition, a new level is created using the highest performing samples in that set as seeds. The process continues recursively on all the new levels. Whilst SuS creates levels in series and chooses seeds as the globally highest performing samples, BSuS creates parallel levels that branch out and chooses the locally best performers as seeds.

The partitions of the input space are created by a function called the *partitioner*. Of course, the choice of partitioner is critical. The details will be provided in Section 4. For now, a generic partitioner is defined as: $\text{PARTITION} : \mathcal{L} \rightarrow \mathbf{Part}(\mathbb{R}^d)$, where $\mathbf{Part}(\mathbb{R}^d)$ denotes the set of all possible partitions of \mathbb{R}^d . During a BSuS run, the partitioner is used on each level after it has been created. If a partition consisting of one set is returned, where that set is necessarily the entire input space, the algorithm carries on as traditional SuS would. If a proper partition of the input space is returned, say A_1, \dots, A_{n_p} , then the algorithm branches out. There will be an independent BSuS run, called a *branch*, started in each set of the partition.

Let \mathbf{X} be the level that caused the branching. For each A_i with $1 \leq i \leq n_p$, the algorithm treats $A_i \cap \mathbf{X}$ as the initial level of the new branch, and creates the next level of the branch in a nearly identical manner to SuS. The only difference is that for a proper partition, $A_i \cap \mathbf{X}$ will have fewer than n samples and so the number of chains is now $p|A_i \cap \mathbf{X}|$. The length of chains remains the same. The Markov chains in each branch are confined to their respective sets using the indicator function $\mathbb{1}_{A_i}(\mathbf{x})$. Note that the indicator function also applies to any branches that this branch might create. From then on, independent BSuS runs take place in each branch. The output of the algorithm is a tree structure T that belongs to the space of all possible trees \mathcal{T} . The nodes of T are triples of the form (\mathbf{X}, A, F) where \mathbf{X} is a level, $A \subset \mathbb{R}^d$ and F is an exceedance region. The *root* of the tree is $(\mathbf{X}^0, \mathbb{R}^d, \mathbb{R}^d)$ where \mathbf{X}^0 is the initial level. If a level \mathbf{X} is created using seeds taken from \mathbf{X}' then \mathbf{X} is a child of \mathbf{X}' .

The BSuS framework offers new options for stopping conditions. Each branch can be considered an independent SuS run and consequently any combination of stopping conditions designed for SuS can be applied to any branch. The most straightforward strategy is to stop the entire algorithm once each individual branch has been stopped. However, there is now the additional possibility of stopping conditions that consider all the branches in parallel. For example, perhaps there is computational budget assigned for evaluating the performance function that cannot be surpassed. In this case, the stopping condition would have to monitor all branches simultaneously. Formally, the stopping conditions now act on \mathcal{T} rather than \mathcal{L} .

In the original SuS algorithm, the level created last is always chosen as the next level to update. In contrast, BSuS must decide between the current branches as to which level will be updated. The numerical examples in this paper use the basic strategy of always choosing the branch that was created first until a stopping condition is triggered. Another simple approach would be to choose the branches uniformly at random. More sophisticated strategies are certainly possible. For instance, the size of the set of interest in each branch could be estimated, and then the branch with largest section could be chosen first. Of course, if a particular BSuS framework is set up in such a way that the branches do not impact one another, the order in which the branches are updated is irrelevant. To reflect that there are many possible choices, a generic choice function will be defined: $\text{CHOOSE} : \mathcal{T} \rightarrow \mathcal{L}$.

The BSuS procedure is summarised in Algorithm 3. There is one minor implementation detail to consider. The way in which the number of chains for each branch was calculated above is only an estimate. Of course, the number of chains has to be an integer, and so the estimate should be rounded. Let the *leaves* be the last level in each branch of a BSuS run. The sum of the number of chains over the leaves should always be equal to np . This rule ensures that the computational complexity of a BSuS run does not unexpectedly blow up. The rounding procedure does not guarantee this, and so some additional check and small adjustment should be performed. It should be noted that sometimes, particularly in cases where there are many branches, a branch will be allotted no chains at all. In this case the branch consists entirely of its initial level, and no new level is created.

3.3. Estimating Exceedance Probabilities

The tree object returned by BSuS can be used to estimate any exceedance probability P_F defined by a threshold b and exceedance region F . The estimation of exceedance probabilities under BSuS is done as follows. Firstly, identify the associated intermediate threshold, say b' , of the associated intermediate exceedance region for each node of T . Delete each node with $b' < b$ and denote the resulting trimmed tree T' . Secondly, number the leaves $1, \dots, n_l$, and for i th leaf, number the nodes on the unique path from the root to the leaf, $(\mathbf{X}_0^i, A_0^i, F_0^i), \dots, (\mathbf{X}_m^i, A_m^i, F_m^i)$. The sequence of levels $\mathbf{X}_0^i, \dots, \mathbf{X}_m^i$ together with the nested sequence of sets $A_0^i \cap F_0^i, \dots, A_m^i \cap F_m^i, A_m^i \cap F$ define a SuS estimator \hat{P}_i for $\mathbb{P}(A_m^i \cap F)$. Since

$$P_F = \mathbb{P}(F) = \sum_{i=1}^{n_l} \mathbb{P}(A_m^i \cap F), \quad (10)$$

it is sensible to suggest

$$\hat{P}_F = \sum_{i=1}^{n_l} \hat{P}_i \quad (11)$$

as an estimator for P_F . Three assumptions are made in the following discussion in order to simplify the analysis of the statistical properties of \hat{P}_F : (i) samples generated by different chains are uncorrelated through the indicator function; (ii) intermediate failure thresholds and partitions are chosen a priori rather than dynamically and (iii) the size of all the levels is a constant n .

It is shown in Appendix A that \hat{P}_F is asymptotically unbiased and consistent by Proposition A.1 and Proposition A.2 respectively. Let the *size* of a SuS estimator be the number of estimators that make up its product. For any i and j , \hat{P}_i and \hat{P}_j can be rewritten as $\hat{P}_i = \hat{P}_{ij} \hat{P}_a$, $\hat{P}_j = \hat{P}_{ij} \hat{P}_b$, where \hat{P}_{ij} , \hat{P}_a , \hat{P}_b are SuS estimators and \hat{P}_{ij} has maximum possible size. It is allowed that $\hat{P}_{ij} = 1$. \hat{P}_{ij} can be thought of as a common root estimator. Let δ_{ij} denote the c.o.v. of \hat{P}_{ij} , which can be estimated by a standard SuS c.o.v.

Algorithm 3 Branching Subset Simulation

InputMinimum level size: $n \in \mathbb{N}$ Level probability: $p \in (0, 1]$ Input distribution: $f: \mathbb{R}^d \rightarrow \mathbb{R}$ Performance function: $g: \mathbb{R}^d \rightarrow \mathbb{R}$ **Definitions** $n_s \leftarrow p^{-1}$ **Subroutines**STOP: $\mathcal{T} \rightarrow \{\mathbf{True}, \mathbf{False}\}$ STEP: $\mathbb{R}^d \rightarrow \mathbb{R}^d$ PARTITION: $\mathcal{L} \rightarrow \mathbf{Part}(\mathbb{R}^d)$ CHOOSE: $\mathcal{T} \rightarrow \mathcal{L}$

```
1: procedure BRANCHINGSUBSETSIMULATION
2:   Sample  $\mathbf{x}_1, \dots, \mathbf{x}_n \sim f(x)$ 
3:    $\mathbf{X} \leftarrow (\mathbf{x}_i)_{i=1}^n$ 
4:   Make  $(\mathbf{X}, \mathbb{R}^d, \mathbb{R}^d)$  root of  $T$ 
5:   while STOP( $T$ ) is False do
6:      $\mathbf{X}, A, F \leftarrow \text{CHOOSE}(T)$ 
7:      $A_1, \dots, A_{n_p} \leftarrow \text{PARTITION}(\mathbf{X})$ 
8:     for  $1 \leq l \leq n_p$  do
9:        $A' \leftarrow A_l \cap A$ 
10:       $n' \leftarrow |A' \cap \mathbf{X}|$ 
11:       $n_c \leftarrow n'p$ 
12:      Let  $\mathbf{x}'_1, \dots, \mathbf{x}'_{n'}$  be a relabelling of  $A' \cap \mathbf{X}$  such that  $g(\mathbf{x}'_1) \geq \dots \geq g(\mathbf{x}'_{n'})$ .
13:       $b \leftarrow g(\mathbf{x}'_{n_c})$ 
14:       $F' \leftarrow \{\mathbf{x} \in \mathbb{R}^d : g(\mathbf{x}) \geq b\}$ 
15:       $f \leftarrow f(\mathbf{x}) \mathbb{1}_{A'}(\mathbf{x}) \mathbb{1}_{F'}(\mathbf{x})$ 
16:      for  $1 \leq i \leq n_c$  do
17:         $\mathbf{x}_{i,1} \leftarrow \mathbf{x}'_i$ 
18:        for  $2 \leq j \leq n_s$  do
19:           $\mathbf{x}_{i,j} \leftarrow \text{STEP}_f(\mathbf{x}_{i,j-1})$ 
20:         $\mathbf{X}' \leftarrow ((\mathbf{x}_{i,j})_{i=1}^{n_c})_{j=1}^{n_s}$ 
21:        Make  $(\mathbf{X}', A', F')$  child of  $(\mathbf{X}, A, F)$ 
22:   return  $T$ 
```

estimator $\hat{\delta}_{ij}$, and $\hat{w}_{ij} = \hat{P}_i \hat{P}_j / \sum_{l,k=1}^{n_l} \hat{P}_l \hat{P}_k$. An estimator for δ , the c.o.v. of BSuS, justified by Proposition A.2 and Proposition A.3, is therefore given by

$$\delta \approx \hat{\delta} = \sqrt{\sum_{i,j=1}^{n_l} \hat{w}_{ij} \hat{\delta}_{ij}^2}. \quad (12)$$

It is also possible to use the output of BSuS to produce $X \sim f|F$ as follows. First, sample $X_i \sim f|A_m^i \cap F$ for $1 \leq i \leq n_l$ using a Markov chain and then randomly pick one of the X_i weighted by $\mathbb{P}(A_m^i \cap F)$. Proposition A.4 shows that the resulting sample will have the required distribution. This is useful for estimating statistics of exceedance regions, like the mean.

4. The Partitioner

4.1. Ergodicity and Convexity

The fundamental improvement BSuS offers over SuS is an increased freedom when selecting seeds. By design, SuS only chooses the highest performing samples as seeds. In contrast, under the BSuS framework, a well designed partitioner of the input space can lead to a seed selection of much better quality. The design of the partitioner will depend on the task BSuS is being applied to (e.g. an optimisation problem may call for a different partitioner than one needed for Bayesian inference). Additionally, there may be varying amounts of information available regarding the performance function, and a good partitioner should efficiently utilise such information. The *Convex Graph Partitioner* (CGP) presented below aims to be widely applicable across different contexts, and assumes the worst case scenario of a computationally expensive black box performance function.

To motivate the CGP, note that the standard definition of convexity is binary: a set $F \subset \mathbb{R}^d$ is either convex or not convex. When this set is endowed with a probability distribution, the way an exceedance region is, it becomes natural to measure whether F is more convex or less convex. The following definition formalises this idea.

Definition 2 (Convexity Measure). Let $F \subset \mathbb{R}^d$ be a set endowed with a distribution with probability density function f . Let $\mathbf{x}, \mathbf{y} \in F$. The convexity measure of F is given as:

$$\mathcal{C}_f(F) = \iint_F f(\mathbf{x})f(\mathbf{y})\chi_F(\mathbf{x}, \mathbf{y})d\mathbf{x}d\mathbf{y}, \quad (13)$$

where

$$\chi_F(\mathbf{x}, \mathbf{y}) = \begin{cases} 1 & \text{if } \{t\mathbf{x} + (1-t)\mathbf{y} : 0 \leq t \leq 1\} \subset F, \\ 0 & \text{otherwise.} \end{cases} \quad (14)$$

It follows immediately from the definition that $0 \leq \mathcal{C}_f(F) \leq 1$. If an exceedance region is convex, its convexity measure is equal to 1. A heuristic governing the CGP can thus be formulated as follows: The lower the convexity measure of an exceedance region, the more likely ergodicity problems will arise when a Markov chain is exploring it. This assertion becomes intuitive when the extreme case is considered. Suppose an exceedance region consists of two disconnected sets that are extremely far apart. Such an exceedance region will have a low convexity measure and cause ergodicity problems. This is because, if a chain is started in one of the disconnected sets, it has a low probability of ever reaching the other set. The CGP aims to reduce the chance of ergodicity problems by partitioning relevant exceedance regions into sets with high convexity measures.

The CGP is itself a modular framework. The first step is to convert the level samples into a graph called the *Convex Graph*. Next, a community detection algorithm is applied to the convex graph, labelling the nodes. Finally, the node labels are transferred to their corresponding level samples and a classifier is trained on the now labelled level. The output of the classifier is a partition of the input space. This process is depicted in Figure 3.

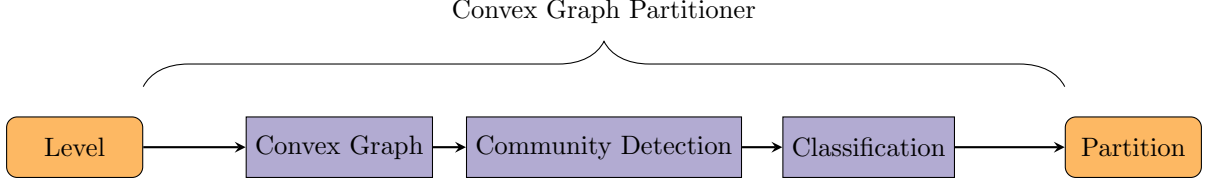


Figure 3: The pipeline of constituent steps of the Convex Graph Partitioner.

4.2. Convexity Graph

Given two samples in a level, say \mathbf{x} and \mathbf{y} , the problem is to decide whether they should belong to the same set of a partition. Suppose that for all exceedance regions that contained \mathbf{x} and \mathbf{y} , they also contained the line segment between \mathbf{x} and \mathbf{y} . According to the above heuristic, it would make sense that \mathbf{x} and \mathbf{y} belong to the same set of a partition, since this would increase the convexity measure of the relevant exceedance regions that intersect with this set. The converse is also true: if for some exceedance region the line segment between \mathbf{x} and \mathbf{y} was not contained within the exceedance region, then the samples should be separate sets, otherwise this would decrease the convexity measure.

A convex graph is a graph that encodes this information. In the next step in the pipeline in Figure 3, the convex graph is partitioned using community detection algorithms. Importantly, community detection algorithms are more likely to assign nodes that are adjacent to the same partition, and thus, samples that according to the above logic should be in the same partition become adjacent.

Definition 3 (Convex Graph). Let $\mathbf{x}_1, \dots, \mathbf{x}_n$ denote all of the samples in a level. For any pair of samples in a level, the smallest exceedance region that contains them both can be defined:

$$F_{ij} = \{\mathbf{x} \in \mathbb{R}^d : g(\mathbf{x}) \geq \min(g(\mathbf{x}_i), g(\mathbf{x}_j))\}. \quad (15)$$

The adjacency matrix of the convex graph is given as

$$A_{ij} = \chi_{F_{ij}}(\mathbf{x}_i, \mathbf{x}_j). \quad (16)$$

Naturally, without explicit access to the performance function, it is impossible to compute the convex graph. Thus, an approximation will be used. The most straightforward approach to approximate A_{ij} is to sample from the line segment connecting \mathbf{x}_i and \mathbf{x}_j and then compute the performance function at each of those sampled points to check whether they lie in F_{ij} . If the performance function is computationally expensive, this approach might not be practical. One option is to train a surrogate performance function on the level samples and then use the surrogate function to sample from the line segment. A simple approach (the one used in the numerical examples in this paper) is to sample once from the midpoint of the line segment and compute the performance. This way, an approximate adjacency matrix can be constructed as follows:

$$\tilde{A}_{ij} = \mathbb{1}_{F_{ij}} \left[\frac{1}{2} (\mathbf{x}_i + \mathbf{x}_j) \right]. \quad (17)$$

Let the *graph budget*, n_e , be number of performance function evaluations required to construct this approximate adjacency matrix. For n samples, n_e is equal to the number of edges in a complete graph of size n , that is

$$n_e = \frac{n(n-1)}{2}. \quad (18)$$

To mitigate computational cost, it is not necessary to use all of the samples from the level. Instead, a random sample can be selected. Thus, by solving Equation 18, n_e becomes a user-defined parameter that determines the number of samples, \tilde{n} , from the current level to be used:

$$\tilde{n} = \left\lceil \frac{1 + \sqrt{1 + 8n_e}}{2} \right\rceil. \quad (19)$$

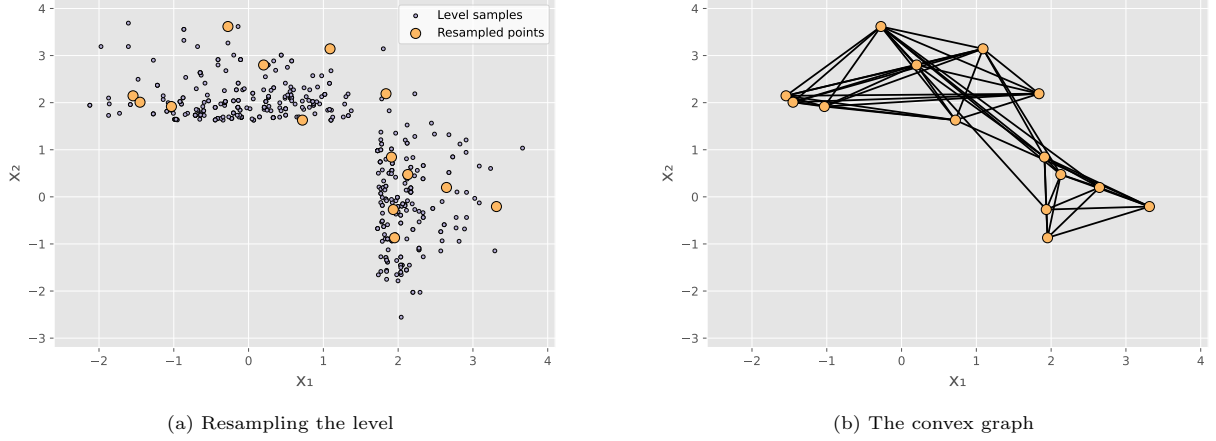


Figure 4: The construction of the convex graph on a level defined with the piecewise linear function. First the vertices are found by sampling from the level, and then the edges are calculated.

If BSuS branches, each branch is assigned a portion of n_e equal to its relative size. The effect the choice of n_e has on the performance of BSuS will be examined in Section 5. The entire process of constructing the convex graph is depicted in Figure 4.

It is very important to note that the above strategy is adopted with potentially high input dimension in mind. Increasing the dimension of the input space does not increase the difficulty of computing the approximate adjacency matrix in Equation 17. Note however that, if instead a surrogate is used to approximate the convex graph, increasing the dimensionality could potentially cause problems when creating the surrogate. The next step in the pipeline, community detection, only considers the graph, and not the coordinates of the samples the nodes represent. Therefore, similarly is not adversely affected by increasing the dimension of the input space.

4.3. Community Detection and Classification

A community of a graph is a set of vertices which is internally densely connected and sparsely connected to the other vertices in the graph. Denote the convex graph, defined by the adjacency matrix of the last step, as $G = (V, E)$, with vertices $V = \{x_1, \dots, x_n\}$. A community of a convex graph represents a region of the input space with high convexity measure, and so should correspond to a set in the final partition. Thus the goal of this step is to find communities using community detection algorithms.

Formally, a community detection algorithm aims to find a partition of V , that is $C_i \subset V$ for $1 \leq i \leq n_p$, such that $C_i \cap C_j = \emptyset$ for $i \neq j$ and $\cup_i C_i = V$. Note that community, label and class can be used interchangeably as terms for denoting which sample belongs to which set of a partition of samples. As previously mentioned, the CGP is a modular framework in the sense that any community detection algorithm could be used. One important consideration when deciding between community detection algorithms is the parameters they require the user to define.

Some community detection algorithms, such as Louvain Community Detection algorithm [17], require the user to specify a resolution parameter. The higher the resolution parameter the more attention that is paid to fine-grained details of the graph and so partitions with more smaller sets are encouraged. The lower the resolution parameter the more the algorithm focuses on large generalised structures of the graph resulting in larger and fewer sets in the partition. Despite the fact that 1 is often used a default value for resolution, there is still the potential for the performance of BSuS to be sensitive to such a parameter. Other options, like the Fluid Communities algorithm [18], require the user to a priori specify the number of communities. If that number is set as 1, the BSuS will never partition and so becomes identical to SuS. However, if that parameter is set as some number greater than 1, the algorithm will partition at every level. This could become an issue since many unnecessary branches can become computationally expensive.

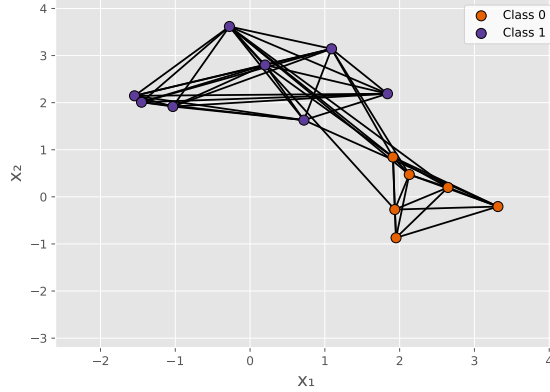


Figure 5: The result of ALP applied to the convex graph. The vertices are separated into two communities.

With the above in mind, the Asynchronous Label Propagation (ALP) algorithm [19] is an attractive option since it does not require the user to specify and parameters. For this reason, ALP is used in the numerical examples of this paper. The details of ALP are given in Appendix B, Section B.1. Regardless of the community detection algorithm used, at the end of this step the labels from the graph are now transferred to the corresponding samples in the input space. Note that since every sample may not have been used when constructing the convex graph, not every sample will at this point receive a label. These samples are simply ignored in the next classification step. The end result of ALP being applied to a convex graph is shown in Figure 5. Now the entire problem has been transformed into the well understood classification problem.

The final step of the CGP is to produce a partition by training a classifier on the now labelled samples. There are of course many different possible choices for classification algorithm and in practice the characteristics of the particular problem will help inform this decision. For the numerical examples in this paper, linear support vector classification (LSVC) is used. The principal reason for this is that LSVC is well suited to high dimensional problems, which are common in the contexts in which SuS is applied. Details of LSVC are given in Appendix B, Section B.2. Figure 6 shows the result of applying LSVC to a labelled level.

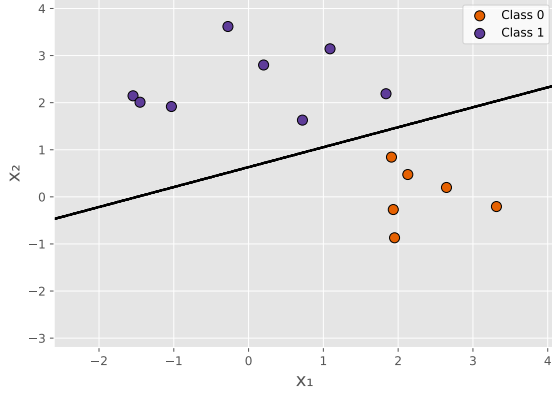
The classification step is the only step of the CGP pipeline that is adversely affected by a high dimensional input space. In this case, it may appropriate to either use dimension reduction techniques before employing a classifier, or to use a classifier that performs well with high dimensional data. In general, a higher graph budget should be chosen for higher dimensions, since this will result in more labelled sampled which in turn makes the classification task easier.

5. Numerical Examples

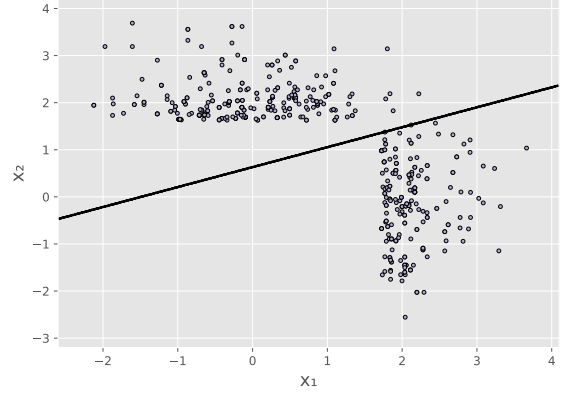
In this section, BSuS is compared to SuS in two contexts where SuS has been successfully applied, namely, reliability analysis and global optimisation. For the purpose of reproducibility, the Python code and data used in this section are available on GitHub at https://github.com/HughKinnear/branching_subset_simulation. The code uses the Scikit-learn LSVC implementation [20] and the NetworkX ALP implementation [21].

5.1. Implementation and Evaluation

Let an *experiment* refer to a set of either 100 SuS or BSuS runs with identical starting parameters. The outcome of each run in an experiment differs only due to the stochastic nature of BSuS and SuS. Let an *experiment setting* be the performance function, stopping conditions and *quality metric* used in an experiment. The quality metric assigns a scalar *quality* to an experiment that measures how desirable the outcome of the experiment is. The quality metric facilitates comparison between BSuS and SuS. The



(a) Partition boundary with labelled samples



(b) Partition boundary with entire level

Figure 6: The partition boundary returned by LSVC applied to a level defined with the piecewise linear function. The classifier is trained on the labelled samples but the final result is that all the level samples are partitioned.

experiment settings in the numerical examples were chosen to reflect the demands of real world problems. In general, if either SuS or BSuS has access to an unlimited computational budget, then an experiment can attain any desired quality for any relevant quality metric. The goal of this section is to show that across a range of different limited computational budgets, BSuS generally attains a better quality than SuS.

In these numerical examples, computational cost was measured by the average number of performance function evaluations over the runs of an experiment, rather than the time taken for a run to terminate. This choice advantages BSuS over SuS, since the community detection and classification steps of the CGP incur a computational cost that is not measured by the number of performance function evaluations. However, the CGP is designed to perform well specifically with a high-dimensional, computationally expensive, black box performance function. In this context, the number of performance function evaluations is a more balanced metric, since together with the Markov chain algorithm, they dominate the computational cost of both BSuS and SuS. Note that the relationship between the number of performance function evaluations and Markov chain steps is similar between SuS and BSuS. In contrast, for illustrative purposes, the performance functions in the numerical examples are simple and 2 dimensional. As a result, the decision to measure the computational cost in this way is a reasonable attempt to emulate an environment for which the CGP is suited. This approach also avoids issues concerning the hardware environment or software implementation of SuS and BSuS.

Given an experiment setting, there are three major ways of influencing the computational cost of SuS and BSuS: level probability, level size and graph budget. A fixed level probability of $p = 0.1$ is used in all the experiments, since it has been shown in the literature [22] that $p \in [0.1, 0.3]$ is optimal. Let an *experiment batch* be a set of experiments that vary only in the level size used. An experiment batch can consist of either experiments made up of SuS runs, or experiments made up of BSuS runs with some fixed graph budget.

For most of the experiments, the parameters of the LSVC algorithm were left as those in the default Scikit-learn 1.3.2 implementation. The most important of these parameters are the penalty function, the loss function and the regularisation parameter, which have the defaults of an L2 penalty function, squared hinge loss, and 1 respectively. Of course, a priori it is not possible to know how to optimally set these parameters, and so in each numerical example a sensitivity analysis is performed using an L1 and L2 penalty function with regularisation values of 0.5, 2, 5, and 10.

In all experiments, both BSuS and SuS used a convergence stopping condition. In particular, a branch or SuS run is stopped if the latest level has constant performance across all of its samples. It is important that BSuS has stopping conditions such as this, since it is possible that branches are created within subsets of the input space which do not allow for other stopping conditions to be triggered. In each numerical example, 50-dimensional performance functions were derived from 2-dimensional performance functions by

adding 48 dummy dimensions. The dummy dimensions have no impact on the output of the performance function. Instead, their purpose is to test how BSuS performs in higher dimensions. Specifically, the dummy dimensions serve as noise, which should decrease the effectiveness of the classifier used by the CGP.

5.2. Reliability Analysis: Piecewise Linear Function

In this experiment setting, each run produces an estimate for the probability of failure, and so each experiment produces 100 such estimates. The piecewise linear function, with accompanying stopping condition and reference probability, is the same that was presented in Section 3.1. The quality metric for this numerical example is the mean squared logarithmic error (MSLE) of these estimates, with respect to the reference probability.

Figure 7 shows a run of BSuS applied to this function. It can be seen that BSuS starts identically to SuS at the initial level. However, at the next level, the partition function returns a partition with two sets. This partition separates the currently high performing samples that will travel in the positive x_2 direction from the currently low performing samples that will eventually travel towards the design point. BSuS is then started again in each set of the partition, allowing them both to be fully explored. The end result is that neighbourhood of the design point is populated, which in turn will lead to a better estimate of the probability of failure, that is without the biased induced by the combination of the greedy nature of SuS and the geometry of the input space.

Figure 8 shows a comparison between the kernel density estimates of the estimates attained from both a SuS experiment and a BSuS experiment, i.e. 100 runs of each. The BSuS estimator is clearly preferable, since more of its probability density is in the neighbourhood of the reference probability. In particular, the right mode of the BSuS estimator has lot more density associated with it than the right mode of the SuS estimator. This implies that BSuS has a higher proportion of runs where the neighbourhood of the design point is populated.

Multiple experiment batches were carried out on both the 2-dimensional and 50-dimensional piecewise linear functions. The MSLE and average number of performance function evaluations was calculated for each experiment. Figure 9 shows the results. For the 2-dimensional case, Figure 9a shows that for a given computational budget, BSuS outperforms SuS across the entire range of level sizes and graph budgets used. For the 50-dimensional case, Figure 9b shows that, even if BSuS performs worse than it does for the 2-dimensional case, it still outperforms SuS across the range of level sizes and graph budgets used for a given computational budget. Note that SuS, with respect to the metrics used, is not affected by the increase in dimension. Figure 10 exhibits a sensitivity analysis on the LSVC parameters with the 50-dimensional performance function. Predictably, the L1 penalty outperforms the L2 penalty since it is able to better ignore the contribution of the irrelevant dimensions. Importantly, for a given computational budget, BSuS still outperforms SuS across the entire range of parameters tested.

5.3. Global Optimisation: Himmelblau's Function

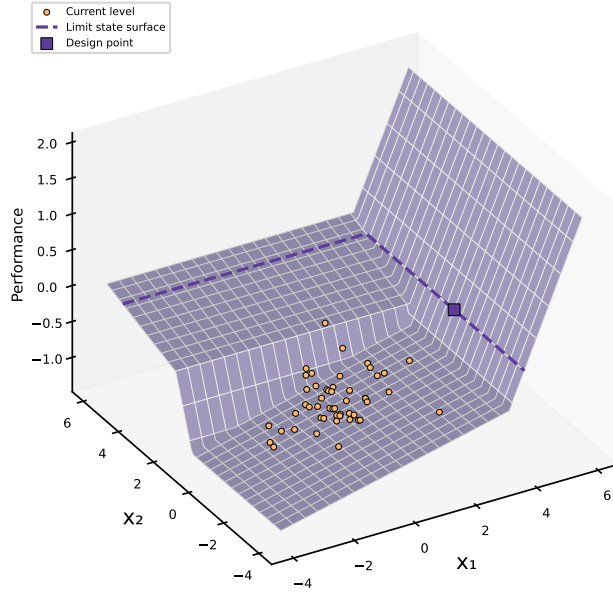
In this setting, the performance function to be optimised is based on Himmelblau's function, a multimodal function often used to test optimisation algorithms [23] given by

$$g(\mathbf{x}) = -((x_1^2 + x_2 - 11)^2 + (x_1 + x_2^2 - 7)^2). \quad (20)$$

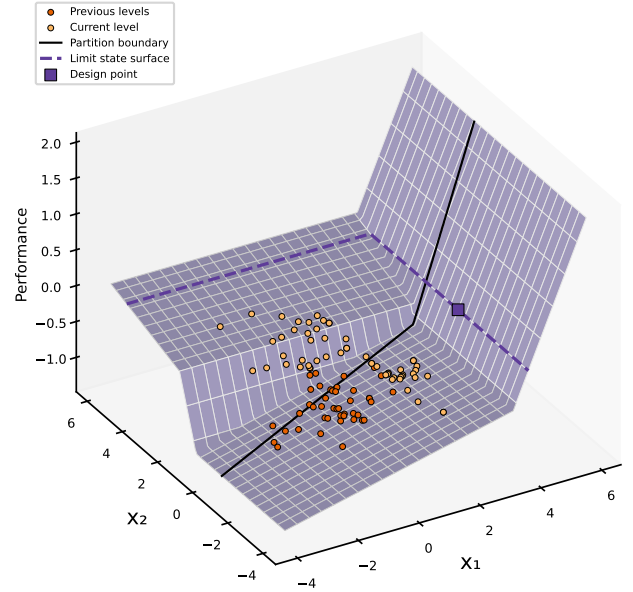
where $\mathbf{x} = (x_1, x_2)^\top$. For the sake of consistency with the proposed algorithm, $g(\cdot)$ is Himmelblau's function multiplied by -1 . The known local maximisers are

$$\begin{aligned} \mathbf{x}_1^* &= (3, 2), \\ \mathbf{x}_2^* &= (-2.805118, 3.131312), \\ \mathbf{x}_3^* &= (-3.779310, -3.283186), \\ \mathbf{x}_4^* &= (3.584428, -1.848126), \end{aligned} \quad (21)$$

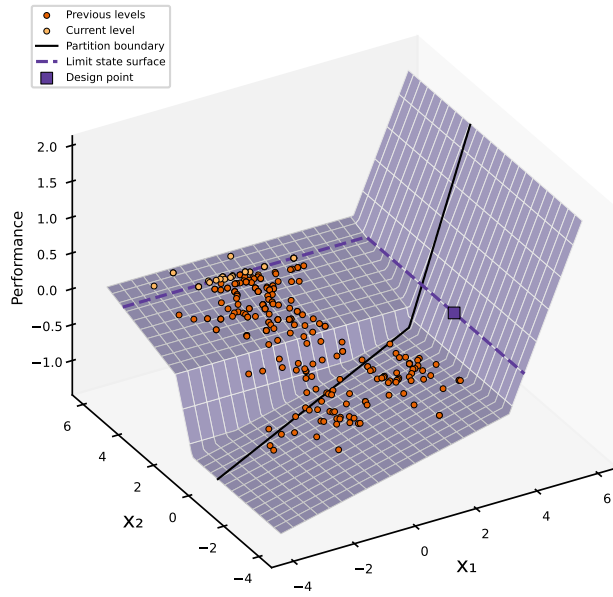
with maximum values $g(\mathbf{x}_i^*) = 0$ for $1 \leq i \leq 4$. Since the local maximisers are at different distances from the origin, SuS tends to only focus on those which are closest to the origin. In particular, very often SuS



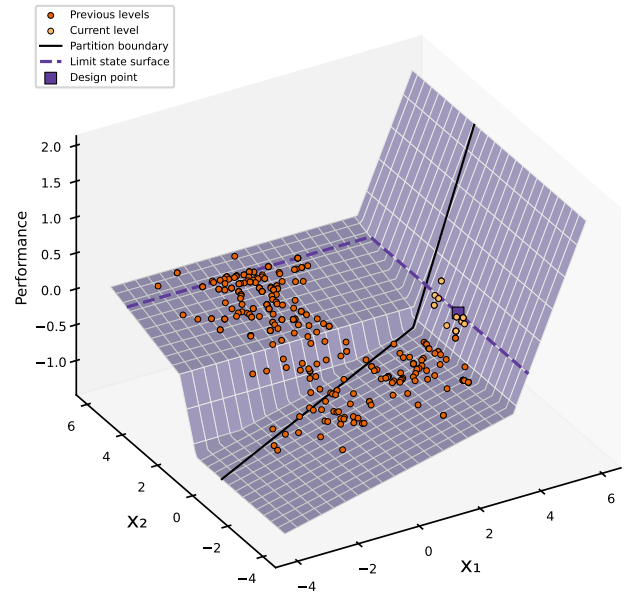
(a) Initial level



(b) Level 1



(c) Level 7



(d) Level 9

Figure 7: BSuS running on the piecewise linear function. For clarity, only every 10th sample has been plotted. BSuS is able to populate the neighbourhood of the design point by partitioning the input space and exploring each set of the partition. The level size is 500 and the graph budget is 50.

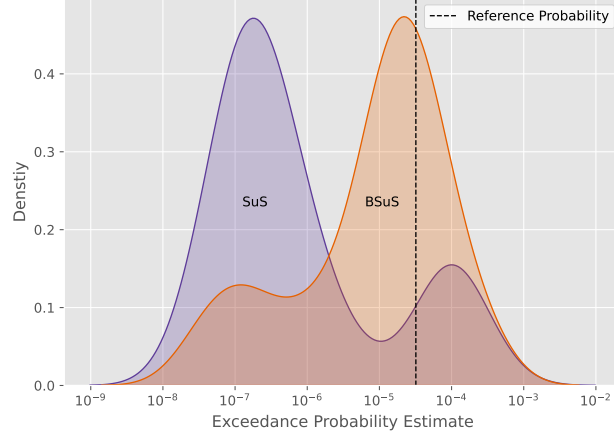
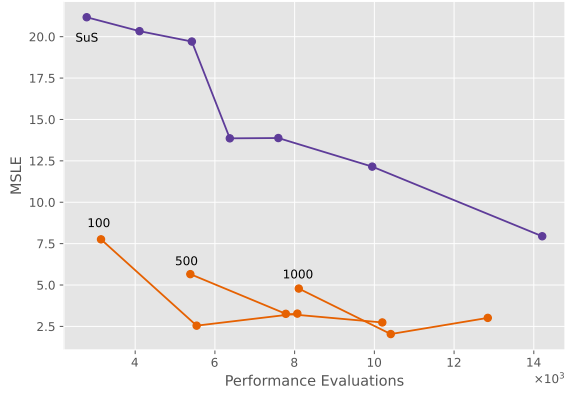
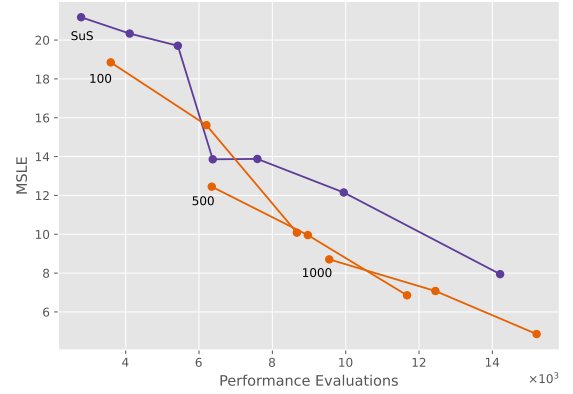


Figure 8: Kernel density estimates of the estimators attained from a SuS experiment and a BSuS experiment on the piecewise linear function. Level size 500 used for both and graph budget 50 used for BSuS.



(a) 2 dimensions



(b) 50 dimensions

Figure 9: Results of experiments on both the 2-dimensional and 50-dimensional piecewise linear function. For both performance functions, four experiment batches were run: one SuS experiment batch with level sizes 500, 750, 1000, 1250, 1500, 2000 and 3000; three BSuS experiment batches with convex budgets 100, 500, and 1000, each made up of experiments with level sizes 500, 1000, 1500. Each point represents an experiment and each line, created using linear interpolation, represents an experiment batch.

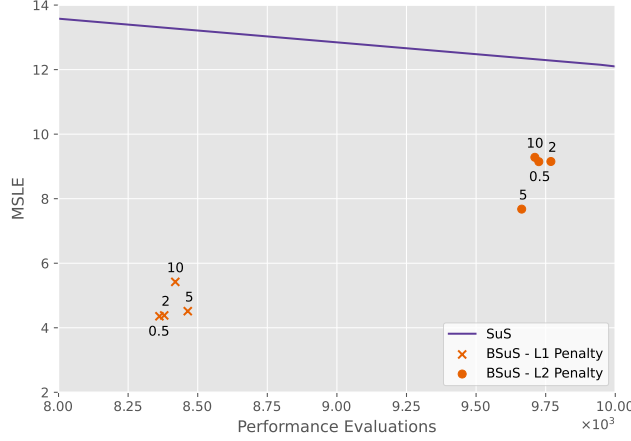


Figure 10: Sensitivity analysis on the LSVC parameters for 50-dimensional piecewise linear function. Each point represents a different experiment with a different set of parameters. A fixed level size of 500 and graph budget of 1000 was used. The points are labelled with the regularisation parameter used. The line representing SuS is the linear interpolation between SuS experiments with different level sizes.

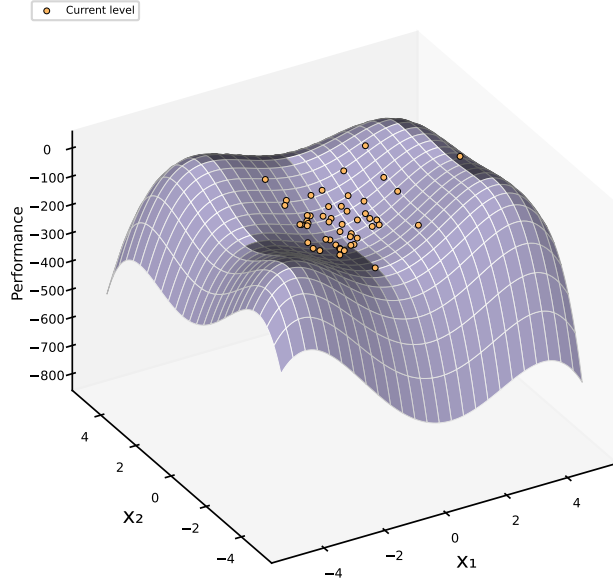
will not find \mathbf{x}_3^* since it is the furthest away. BSuS should eventually create a partition containing each of the local maximisers and then proceed to find each one. Aside from the convergence stopping condition, no additional stopping conditions were used in this numerical example. This because in optimisation problems the maximum performance may not be available. The quality metric used for this numerical example is the average number of maximum values found. That is, after each run has ended, one counts how many of the four maximum points have at least one sample within a $1/4$ Euclidean radius. Then, the quality metric is the average of these counts across the whole experiment.

In Figure 11, a single run is presented to demonstrate why BSuS is expected to outperform SuS on this quality metric. The first partition is shown in Figure 11b, in which the partition contains 3 sets. Note that two of the sets contain one maximiser each, but one of the sets contains two maximisers. For the sets with one maximiser, BSuS is almost guaranteed to find the maximum point. For the set with two maximisers, there is a chance BSuS only finds one of them. Figure 11c shows the second partition, which splits the set containing two maximisers into two sets, each containing one maximiser. The final result is four branches, each corresponding to a maximiser. Finally, each maximiser is found and the stopping condition is triggered in each branch.

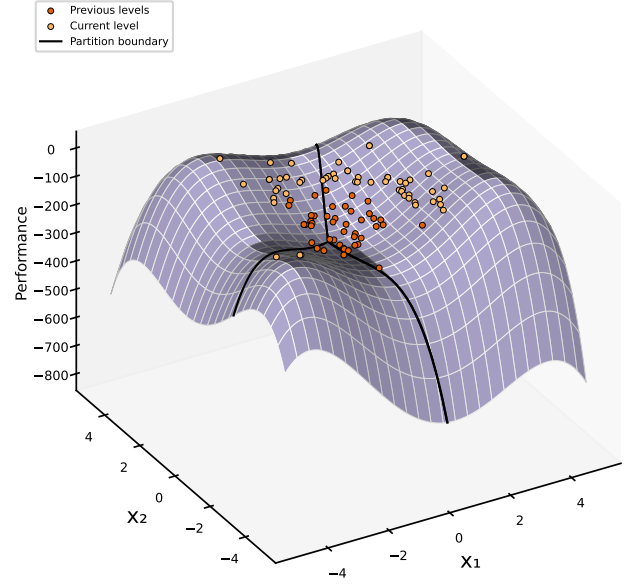
Multiple experiment batches were carried out on both the 2-dimensional and 50-dimensional versions of the objective function. The average number of maximal points found and average number of performance function evaluations was calculated for each experiment. Figure 12 shows the results. For the 2-dimensional case, Figure 12a shows that for a given computational budget, BSuS outperforms SuS across the entire range of level sizes and graph budgets used. In particular, BSuS has a large advantage with the higher computational budgets. For the 50-dimensional case, Figure 12b shows that BSuS performs worse than it does for the 2-dimensional case. However, for all cases except one it outperforms SuS across the range of level sizes and graph budgets used for a given computational budget. Figure 13 shows a sensitivity analysis on the LSVC parameters with the 50-dimensional performance function. Again, predictably the L1 penalty outperforms the L2 penalty. Importantly, for a given computational budget, BSuS still outperforms SuS across the entire range of parameters tested.

6. Conclusion

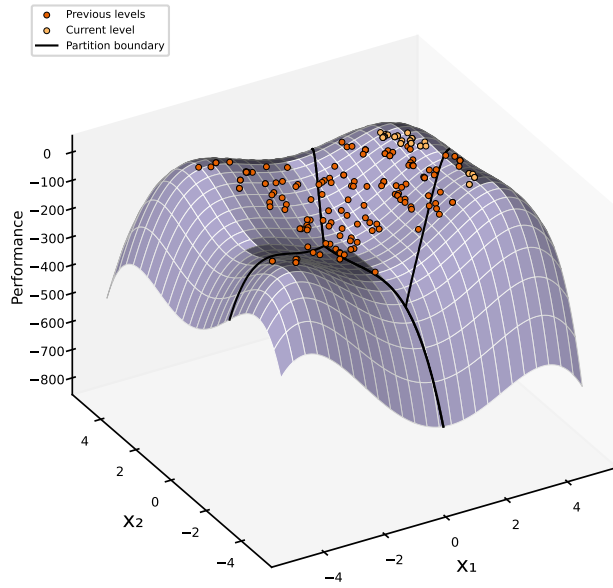
This paper presented BSuS, a recursively branching framework for rare-event simulation. BSuS retains the advantageous features of SuS, one of the most widespread rare-event simulation algorithms. These features include the efficient sampling which has made SuS widely applicable in contexts such as reliability



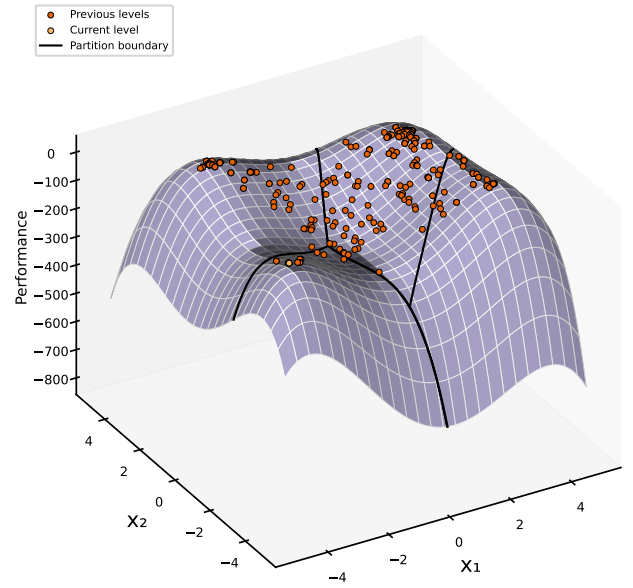
(a) Initial level



(b) Level 1

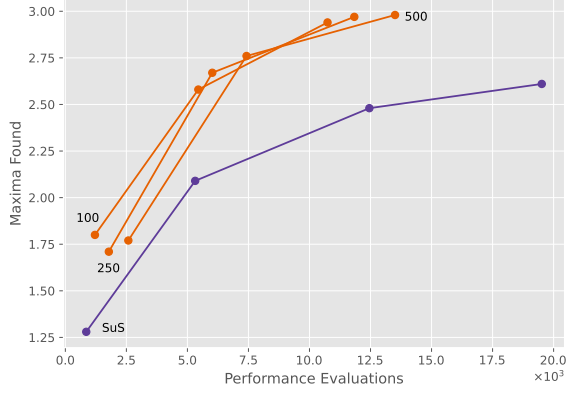


(c) Level 5

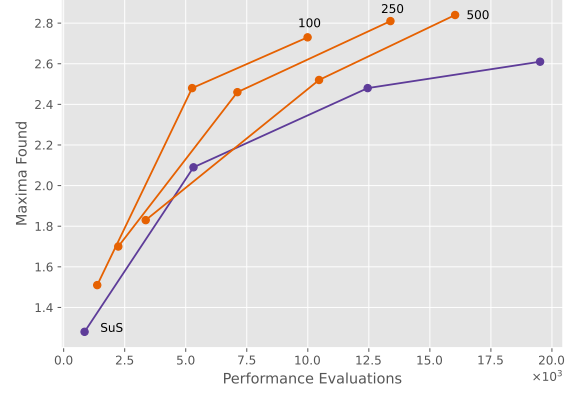


(d) Level 19

Figure 11: BSuS running on Himmelblau's function. For clarity, only every 10th sample has been plotted. The level size is 500 and the graph budget is 50.



(a) 2 dimensions



(b) 50 dimensions

Figure 12: Results of experiments on both the 2-dimensional and 50-dimensional Himmelblau's function. For both performance functions, four experiment batches were run: one SuS experiment batch with level sizes 100, 500, 1000, and 1500; three BSuS experiment batches with convex budgets 100, 250, and 500, each made up of experiments with level sizes 100, 500 1000. Each point represents an experiment and each line, created using linear interpolation, represents an experiment batch.

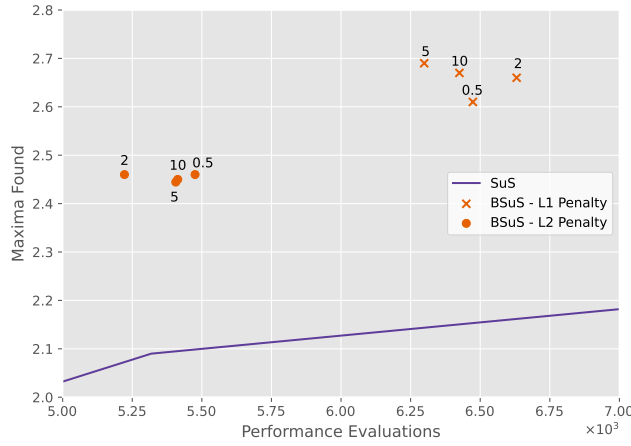


Figure 13: Sensitivity analysis on the LSVC parameters for 50-dimensional Himmelblau's function. Each point represents a different experiment with a different set of parameters. A fixed level size of 500 and graph budget of 50 was used. The points are labelled with the regularisation parameter used. The line representing SuS is the linear interpolation between SuS experiments with different level sizes.

analysis and global optimisation. At the same time, BSuS offers greater resilience to ergodicity problems caused by the greedy nature of SuS and the geometry of the input space. BSuS achieves this by dynamically partitioning the input space to allow for a more efficient exploration. The BSuS framework is modular and allows the user to tailor its elements, namely the partitioner, stopping conditions and branch selection scheme. The details of the framework were introduced, and it was shown with numerical examples that BSuS outperforms SuS across a broad range of parameter values.

Future research will improve resource allocation between branches. Currently, it is possible for some branches to be prematurely stopped, since it is possible that they are not assigned sufficient Markov chains at the initial branching. This can be problematic when there are a large number of branches, which could be the result of a highly multimodal performance function. There are also opportunities for improvement in the branch selection scheme, such that the most promising branches are updated first.

Appendix A. Statistical Properties of BSuS

Proposition A.1. *If an estimator \hat{P} of P is the sum of SuS estimators based on levels of size n , $\hat{P} = \sum_{t=1}^T \hat{P}_t$, where \hat{P}_t is estimating P_t and $P = \sum_{t=1}^T P_t$, then*

$$\left| \mathbb{E} \left[\frac{\hat{P} - P}{P} \right] \right| = O(1/n). \quad (\text{A.1})$$

Thus \hat{P} is asymptotically unbiased.

PROOF.

$$\begin{aligned} \left| \mathbb{E} \left[\frac{\hat{P} - P}{P} \right] \right| &= \left| \mathbb{E} \left[\frac{\sum_{t=1}^T \hat{P}_t - P}{\sum_{t=1}^T P_t} \right] \right| \\ &\leq \left| \mathbb{E} \left[\sum_{t=1}^T \frac{\hat{P}_t - P_t}{P_t} \right] \right| \\ &= \left| \sum_{t=1}^T \mathbb{E} \left[\frac{\hat{P}_t - P_t}{P_t} \right] \right| \\ &\leq \sum_{t=1}^T \left| \mathbb{E} \left[\frac{\hat{P}_t - P_t}{P_t} \right] \right| \\ &= O(1/n) \end{aligned}$$

where the last step is justified since the bias of a SuS estimator is $O(1/n)$ [1].

Proposition A.2. *If an estimator \hat{P} of P is the sum of SuS estimators based on levels of size n , $\hat{P} = \sum_{t=1}^T \hat{P}_t$, where \hat{P}_t is estimating P_t , $P = \sum_{t=1}^T P_t$ and δ is the c.o.v. of \hat{P} , then*

$$\delta^2 = \mathbb{E} \left[\frac{\hat{P} - P}{P} \right]^2 = \sum_{i,j=1}^T w_{ij} \delta_i \delta_j \rho_{ij} = O(1/n), \quad (\text{A.2})$$

where $w_{ij} = P_i P_j / \sum_{l,k=1}^T P_l P_k$, δ_t is the c.o.v. of \hat{P}_t and ρ_{ij} is the correlation between \hat{P}_i and \hat{P}_j . It follows that \hat{P} is a consistent estimator.

PROOF.

$$\begin{aligned} \mathbb{E} \left[\frac{\hat{P} - P}{P} \right]^2 &= \mathbb{E} \left[\frac{(\sum_{t=1}^T \hat{P}_t - P)^2}{(\sum_{t=1}^T P_t)^2} \right] \\ &= \mathbb{E} \left[\frac{\sum_{i,j=1}^T (\hat{P}_i - P_i)(\hat{P}_j - P_j)}{\sum_{i,j=1}^T P_i P_j} \right] \\ &= \mathbb{E} \left[\sum_{i,j=1}^T w_{ij} \frac{(\hat{P}_i - P_i)(\hat{P}_j - P_j)}{P_i P_j} \right] \\ &= \sum_{i,j=1}^T w_{ij} \delta_i \delta_j \rho_{ij} \\ &= O(1/n) \end{aligned}$$

where the last step is justified since the c.o.v. of a SuS estimator is $O(1/\sqrt{n})$ [1].

Proposition A.3. If $\hat{P}_1 = \hat{P}\hat{P}_a$, $\hat{P}_2 = \hat{P}\hat{P}_b$ are estimators where \hat{P}_a, \hat{P}_b , and \hat{P} are pairwise independent, δ, δ_1 , and δ_2 are the respective c.o.v. variables and ρ is the correlation between \hat{P}_1 and \hat{P}_2 , then

$$\delta_1 \delta_2 \rho = \delta^2. \quad (\text{A.3})$$

PROOF.

$$\begin{aligned} \delta_1 \delta_2 \rho &= \frac{\mathbb{E}[\hat{P}^2 \hat{P}_a \hat{P}_b] - \mathbb{E}[\hat{P} \hat{P}_a] \mathbb{E}[\hat{P} \hat{P}_b]}{\mathbb{E}[\hat{P}_1] \mathbb{E}[\hat{P}_2]} \\ &= \frac{\mathbb{E}[\hat{P}_a] \mathbb{E}[\hat{P}_b] (\mathbb{E}[\hat{P}^2] - \mathbb{E}[\hat{P}]^2)}{\mathbb{E}[\hat{P}_a] \mathbb{E}[\hat{P}_b] \mathbb{E}[\hat{P}]^2} \\ &= \delta^2 \end{aligned}$$

Proposition A.4. Let $X \sim F_X$, A_1, \dots, A_n be a partition of the sample space, $X_i \sim X|A_i$, $\theta = (\theta_1, \dots, \theta_n) \sim \text{Multinomial}(1; \mathbb{P}(A_1), \dots, \mathbb{P}(A_n))$ and $Y = \sum_{i=1}^n \theta_i X_i \sim F_Y$. Then X and Y are identically distributed.

PROOF.

$$\begin{aligned} F_Y(y) &= \mathbb{P}(Y \leq y) \\ &= \mathbb{P}\left(\sum_{i=1}^n \theta_i X_i \leq y\right) \\ &= \sum_{i=1}^n \mathbb{P}(X_i \leq y) \mathbb{P}(\theta_i = 1) \\ &= \sum_{i=1}^n \mathbb{P}(X \leq y | X \in A_i) \mathbb{P}(A_i) \\ &= \mathbb{P}(X \leq y) \\ &= F_X(y) \end{aligned}$$

Appendix B. Convex Graph Partitioner

B.1. Asynchronous Label Propagation

Denote a graph as $G = (V, E)$, with vertices $V = \{x_1, \dots, x_n\}$. ALP updates the labels of the vertices iteratively through different discrete time steps. Let $C_{x_i}(t)$ denote the label of x_i at time t . At the beginning of the algorithm each sample is assigned its own unique label, that is $C_{x_i}(0) = i$. To obtain the labels at step t given the labels at step $t-1$, first the vertices are given a random ordering in which they shall be updated. Let n_i be the number of vertices adjacent to x_i . In the specified order, node x_i is updated with following rule:

$$C_{x_i}(t) = h(C_{x_{i1}}(t), \dots, C_{x_{im}}(t), C_{x_{i(m+1)}}(t-1), \dots, C_{x_{in_i}}(t-1)), \quad (\text{B.1})$$

where x_{i1}, \dots, x_{im} are the vertices adjacent to x_i that have already been updated, $x_{i(m+1)}, \dots, x_{in_i}$ are the vertices adjacent to x_i that are still awaiting an update for this iteration, and h is function that returns the most common label. In the event of a tie, h picks a label amongst those tied uniformly at random. Due to this tie breaking procedure it is inappropriate to have a stopping condition that looks for no label changes in an iteration, since it is always possible for some labels to change if there is a tie. Consequently, instead the algorithm stops if every vertex has a label that is amongst those labels that have caused a tie.

B.2. Linear Support Vector Machine

Since it is possible for there to be more than two classes in the context of the CGP, a one-vs-the-rest strategy is required, in which a classifier is created for each class. Formally, given a class, let $(\mathbf{x}_i, y_i)_{i=1}^n$ be the labelled samples, where $y_i = 1$ if x_i is in the class and $y_i = -1$ otherwise. Now a confidence score is assigned to each sample, $\mathbf{w}^T \mathbf{x}_i + b$, where the coefficients $\mathbf{w} \in \mathbb{R}^d$ and intercept $b \in \mathbb{R}$ are determined by the following optimisation problem:

$$\min_{\mathbf{w}, b} \frac{1}{2} \rho(\mathbf{w}) + C \sum_{i=1}^n \max(0, 1 - y_i(\mathbf{w}^T \mathbf{x}_i + b))^2, \quad (\text{B.2})$$

where ρ is a penalty function and C is regularisation parameter. Possible penalty functions include the L1 penalty, $\rho(\mathbf{w}) = \|\mathbf{w}\|_1$, and the L2 penalty, $\rho(\mathbf{w}) = \|\mathbf{w}\|_2^2$. Once this process has been completed for each class, each sample can be labelled according to whichever classifier gives it the largest confidence score.

References

- [1] S. K. Au, J. L. Beck, Estimation of small failure probabilities in high dimensions by subset simulation, *Probabilistic Engineering Mechanics* 16 (4) (2001) 263–277. doi:10.1016/S0266-8920(01)00019-4.
- [2] D. Straub, I. Papaioannou, Bayesian Updating with Structural Reliability Methods, *Journal of Engineering Mechanics* 141 (3) (2015) 04014134. doi:10.1061/(ASCE)EM.1943-7889.0000839.
- [3] F. A. DiazDelaO, A. Garbuno-Inigo, S. K. Au, I. Yoshida, Bayesian updating and model class selection with Subset Simulation, *Computer Methods in Applied Mechanics and Engineering* 317 (2017) 1102–1121. doi:10.1016/j.cma.2017.01.006.
- [4] W. Betz, I. Papaioannou, J. L. Beck, D. Straub, Bayesian inference with Subset Simulation: Strategies and improvements, *Computer Methods in Applied Mechanics and Engineering* 331 (2018) 72–93. doi:10.1016/j.cma.2017.11.021.
- [5] M. Chiachio, J. L. Beck, J. Chiachio, G. Rus, Approximate Bayesian Computation by Subset Simulation, *SIAM Journal on Scientific Computing* 36 (3) (2014) A1339–A1358. doi:10.1137/130932831.
- [6] H.-S. Li, Subset simulation for unconstrained global optimization, *Applied Mathematical Modelling* 35 (10) (2011) 5108–5120. doi:10.1016/j.apm.2011.04.023.
- [7] Z. T. Gong, F. A. DiazDelaO, P. O. Hristov, M. Beer, History Matching with Subset Simulation, *International Journal for Uncertainty Quantification* 11 (5) (2021) 19–38. doi:10.1615/Int.J.UncertaintyQuantification.2021033543.
- [8] K. Breitung, The geometry of limit state function graphs and subset simulation: Counterexamples, *Reliability Engineering & System Safety* 182 (2019) 98–106. doi:10.1016/j.ress.2018.10.008.
- [9] A. Abdollahi, M. Azhdary Moghaddam, S. A. Hashemi Monfared, M. Rashki, Y. Li, Subset simulation method including fitness-based seed selection for reliability analysis, *Engineering with Computers* 37 (4) (2021) 2689–2705. doi:10.1007/s00366-020-00961-9.
- [10] M. Rashki, SESC: A new subset simulation method for rare-events estimation, *Mechanical Systems and Signal Processing* 150 (2021) 107139. doi:10.1016/j.ymssp.2020.107139.
- [11] P. R. Wagner, S. Marelli, I. Papaioannou, D. Straub, B. Sudret, Rare event estimation using stochastic spectral embedding, *Structural Safety* 96 (2022) 102179. doi:10.1016/j.strusafe.2021.102179.
- [12] I. Papaioannou, W. Betz, K. Zwirgmaier, D. Straub, MCMC algorithms for Subset Simulation, *Probabilistic Engineering Mechanics* 41 (2015) 89–103. doi:10.1016/j.pro bengmech.2015.06.006.
- [13] Z. Wang, M. Broccardo, J. Song, Hamiltonian Monte Carlo methods for Subset Simulation in reliability analysis, *Structural Safety* 76 (2019) 51–67. doi:10.1016/j.strusafe.2018.05.005.
- [14] L. Katafygiotis, K. Zuev, Geometric insight into the challenges of solving high-dimensional reliability problems, *Probabilistic Engineering Mechanics* 23 (2008) 208–218. doi:10.1016/j.pro bengmech.2007.12.026.
- [15] M. Rosenblatt, Remarks on a Multivariate Transformation, *The Annals of Mathematical Statistics* 23 (3) (1952) 470–472. doi:10.1214/aoms/1177729394.
- [16] A. Nataf, Determination des distributions dont les marges sont donnees., *C. R. Acad. Sci. Paris* (225) (1962) 42–43.
- [17] V. D. Blondel, J.-L. Guillaume, R. Lambiotte, E. Lefebvre, Fast unfolding of communities in large networks, *Journal of Statistical Mechanics: Theory and Experiment* 2008 (10) (2008) P10008. doi:10.1088/1742-5468/2008/10/P10008.
- [18] F. Parés, D. G. Gasulla, A. Vilalta, J. Moreno, E. Ayguadé, J. Labarta, U. Cortés, T. Suzumura, Fluid Communities: A Competitive, Scalable and Diverse Community Detection Algorithm, in: C. Cherifi, H. Cherifi, M. Karsai, M. Murolesi (Eds.), *Complex Networks & Their Applications VI*, Studies in Computational Intelligence, Springer International Publishing, Cham, 2018, pp. 229–240. doi:10.1007/978-3-319-72150-7_19.
- [19] U. N. Raghavan, R. Albert, S. Kumara, Near linear time algorithm to detect community structures in large-scale networks, *Physical Review E* 76 (3) (2007) 036106. doi:10.1103/PhysRevE.76.036106.
- [20] M. Feurer, K. Eggenberger, S. Falkner, M. Lindauer, F. Hutter, Practical Automated Machine Learning for the AutoML Challenge 2018, *International Workshop on Automatic Machine Learning at ICML* (2018) 12.
- [21] A. A. Hagberg, D. A. Schult, P. J. Swart, Exploring network structure, dynamics, and function using NetworkX, in: G. Varoquaux, T. Vaught, J. Millman (Eds.), *Proceedings of the 7th Python in Science Conference*, Pasadena, CA USA, 2008, pp. 11–15.
- [22] K. M. Zuev, J. L. Beck, S.-K. Au, L. S. Katafygiotis, Bayesian post-processor and other enhancements of Subset Simulation for estimating failure probabilities in high dimensions, *Computers & Structures* 92–93 (2012) 283–296. doi:10.1016/j.compstruc.2011.10.017.
- [23] D. M. Himmelblau, *Applied Nonlinear Programming*, McGraw-Hill, 1972.